Dalton Transactions

RSC Publishing

PAPER

View Article Online
View Journal | View Issue

Cite this: *Dalton Trans.*, 2013, **42**, 6110

Discrimination of fluorescence light-up effects induced by pH and metal ion chelation on a spirocyclic derivative of rhodamine B†

Andreia Leite,[a] Ana M. G. Silva,*[a] Luís Cunha-Silva,[a] Baltazar de Castro,[a] Paula Gameiro[a] and Maria Rangel*[b]

In the present work we describe the structure and the spectroscopic characterization of a spirocyclic derivative of a rhodamine B ligand whose properties allow discrimination of light-up effects induced by metal ion chelation and variation of pH. Distinction of the two effects is important for the use of this type of ligand to detect and monitor metal ions in aqueous solutions. The synthesis of the ligand was performed in two steps, which involve the reaction of rhodamine B with hydrazine hydrate to form rhodamine B hydrazide followed by condensation with 2-pyridinecarboxaldehyde and was successfully optimized using a solvent free approach under microwave irradiation. The ligand was obtained in the expected spirolactam form and was characterized in the solid state by EA, MS and single-crystal X-ray diffraction. The ligand was characterized in solution by NMR and absorption and fluorescence spectroscopies and its properties were found to be sensitive to pH and concentration of iron(III). The study of the fluorescence properties at variable pH shows that the compound is fluorescent in the range 2 < pH < 4 with maximum intensity at pH 3 and allowed the determination of two pK_a values (pK_{a1} = 2.98, pK_{a2} = 2.89) and establishment of the corresponding distribution diagram. The very low pK_a values guarantee that above pH equal to 4 the ligand is mostly present in the fully non-protonated and non-fluorescent form L. The study of the interaction of the ligand with iron(III) was performed in DMSO and DMSO–H_2O to exclude the influence of pH and due to the low solubility of the compound. The results indicate that the presence of iron(III) triggers the opening of the spirolactam form of the ligand and the maximum intensity obtained at a metal : ligand ratio of 1 : 2 is consistent with the formation of an iron(III) complex with the tridentate ligand.

Received 21st September 2012,
Accepted 11th December 2012

DOI: 10.1039/c2dt32198j

www.rsc.org/dalton

Introduction

Metal ions play important roles in biochemical processes and regulation of their metal ion concentration is crucial for life. Consequently one of the main goals in the field of chemical sensors is the detection and quantification of those two relevant metal ions.[1]

Fluorescence spectroscopy is a highly sensitive technique that allows real time information on the localization and quantification of the analytical targets. In the last few years several fluorescent ligands with different photophysical properties have been used to identify and measure metal ions in several types of matrices. Dyes of the xanthene family are amongst the most used fluorescent ligands due to their excellent properties, such as high extinction coefficient, high quantum yield and photostability. At present, most of the chemical sensors in use are based on the measurement of the quenching observed in fluorescence intensity in the presence of metal ions. These methodologies usually require the use of a de-quencher agent to validate the results and do not provide a positive signal in microscopy methods.[2]

More recently, a strong effort has been put on the design of 'turn-on' sensors, in which silent molecules are activated in the presence of metal ions. The spirocyclic derivatives of rhodamine have proved to be useful sensing platforms since the ring-opening process leads to a fluorescence light-up effect of the ligand.[3] Several procedures have been developed to prepare spirocyclic rhodamines and the use of derivatives of

[a]*REQUIMTE, Departamento de Química e Bioquímica, Faculdade de Ciências, Universidade do Porto, 4169-007 Porto, Portugal. Fax: +351 220402659; Tel: +351 220402593*

[b]*REQUIMTE, Instituto de Ciências Biomédicas de Abel Salazar, 4099-003 Porto, Portugal. E-mail: mcrangel@fc.up.pt, mrangel@icbas.up.pt*

† Electronic supplementary information (ESI) available: Synthesis using conventional heating protocol, NMR spectra, additional crystal structure figures and interaction of ligand **L** with Fe^{3+}, Fe^{2+}, Cu^{2+} and Zn^{2+}. CCDC 901532. For ESI and crystallographic data in CIF or other electronic format see DOI: 10.1039/c2dt32198j

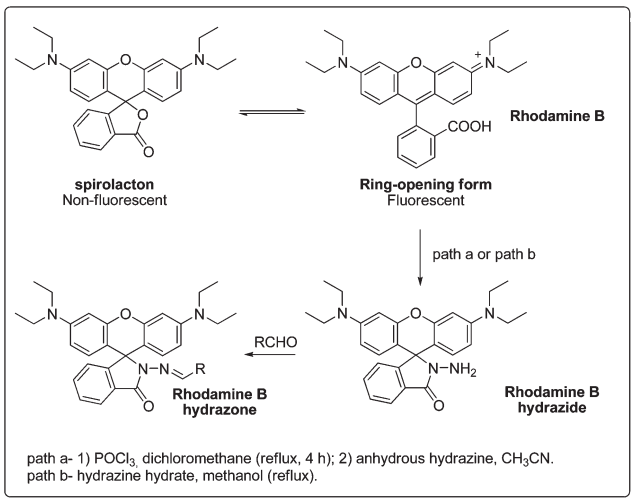

Scheme 1 Synthetic routes to prepare rhodamine B hydrazide derivatives.

rhodamine B hydrazide is one example. This highly versatile and useful rhodamine B hydrazide was first prepared by Czarnik and co-workers in 80% yield, through the reaction of rhodamine B with $POCl_3$ in dichloroethane followed, without purification, by the reaction with anhydrous hydrazine, and evaluated as a chemodosimeter for Cu(II) (Scheme 1, path a).[4] Later, Yang and co-workers employed a different strategy to synthesise the same molecule, *via* a one-step reaction of rhodamine B with hydrazine hydrate in methanol under reflux (68% yield), and demonstrated its potentiality as a fluorogenic ligand for determination of peroxynitrite (Scheme 1, path b).[5]

Thereafter, a large number of papers involving fluorescent ligands based on spiro ring-opening processes have been published and recently reviewed by Yoon and co-workers.[3,6]

The modification of the rhodamine derivatives was most commonly concentrated on the N-terminus of spirolactam, which was linked to various receptors for targets of interest, such as metal ions, thiols, ROS/RNS, organophosphates, *etc.* In fact, a number of ligands having receptors with different coordination spheres have been prepared through the condensation of rhodamine B hydrazide with a variety of aldehydes, following the synthetic strategy present in Scheme 1. The ligands based on the rhodamine B hydrazide scaffold further explored to date were specifically developed for the detection and measurement of Cu^{2+} metal ions and result from the condensation with the aldehydes: (i) 8-hydroxy-2-quinolinecarboxaldehyde;[7] (ii) 2,4-dihydroxybenzaldehyde;[8] (iii) methyl-5-formyl-1*H*-pyrrole-2-carboxylate;[9] (iv) (*R*)-2,20-dihydroxy-1,10-binaphthyl-3-carbaldehyde, 2-hydroxy-1-naphthaldehyde and 2-methoxybenzaldehyde;[10] (v) (*S*)-3-formyl-2,2′-binaphthyl-20-crown-6 and (*S*)-2,2′-dihydroxy-[1,1′-binaphthalene]-3,3′-dicarboxaldehyde;[11] (vi) 2-formylphenylboronic acid;[12] (vii) glyoxal and then N_2S_2 [13] and (viii) *p*-dimethylaminobenzaldehyde.[14] However, a few ligands have been developed for Pd^{2+}, Hg^{2+} and Fe^{3+} metal ions.[15–17]

Beyond the modifications of the rhodamine B hydrazide, other approaches based on spirocyclic derivatives of rhodamines have been explored.[18–21] However the great majority of these processes have been carried out using conventional oil-bath heating, at high temperatures in order to perform the reactions within a reasonable timeframe. It has been shown that controlled microwave heating under closed-vessel conditions dramatically reduces the reaction time; increases product yields and purity of the product by reducing unwanted side reactions.[22] To the best of our knowledge no examples have been reported exploring the synthesis of spirocyclic derivatives of rhodamine using this advanced heating methodology.

Also, one of the more important questions raised by the utilization of this type of ligands to detect and monitor metal ions in aqueous media is the assurance of discrimination between a fluorescence light-up effect produced by metal ion chelation or variation of the pH value.[45]

In this work, we report the improved synthesis and characterization of a 'turn-on' ligand previously reported by Mandal and co-workers.[23] This is the first example of a microwave-assisted synthesis of a 'turn-on' fluorescent chelator based on the lipophilic rhodamine B molecule whose fluorescence is triggered in the presence of iron(III) as a result of the opening of the spirolactam form.

The structure of the ligand was resolved by X-ray diffraction. Fluorescence studies in solution at variable pH and different metal/ligand ratios allowed the determination of the pK_a values of the ligand and discrimination between pH and iron(III) "fluorescence light-up" effects. The very low pK_a values guarantee that above pH equal to 4 the ligand is mostly present in the fully non-protonated and non-fluorescent form L thus denoting that the opening of the spirolactam form and consequently the fluorescence 'turn-on' effect can only arise from chelation of a metal ion.

Experimental section

Materials and methods

Reagents and solvents were purchased as reagent-grade and used without further purification unless otherwise stated.

NMR spectra were recorded with a Bruker Avance III 400 spectrometer (400.15 MHz for ^1H and 100.63 MHz for ^{13}C). Chemical shifts (δ) are reported in ppm and coupling constants (J) in Hz; internal standard was TMS. Unequivocal ^1H assignments were made with the aid of 2D gCOSY ($^1H/^1H$), while ^{13}C assignments were made on the basis of 2D gHSQC ($^1H/^{13}C$) and gHMBC experiments (delay for long range J C/H couplings was optimized for 7 Hz). Mass spectra and microanalysis were acquired by Unidade de Espectrometría de Masas and Unidade de Análise Elemental, both from Santiago de Compostela. Microwave-assisted reactions were carried out in a CEM Discovery Labmate circular single-mode cavity instrument (300 W max magnetron power output) from CEM Corporation.

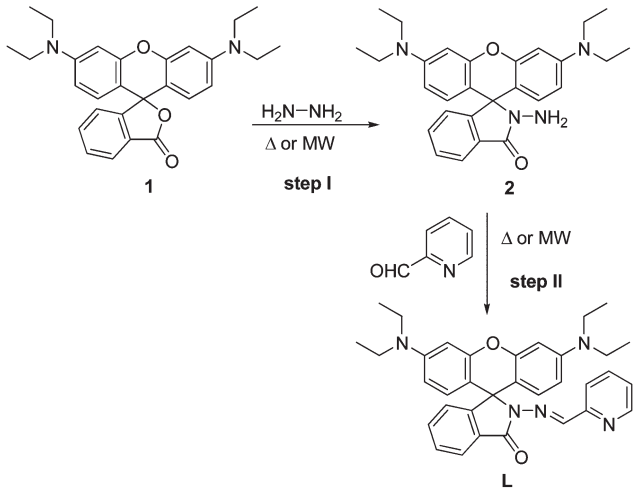

Scheme 2 Synthetic route for the preparation of ligand **L**.

Table 1 Step I experiments to prepare rhodamine B hydrazide (**2**) using different heating methods

Entry	Method	Temp. [°C]	Time (min)	Yield[a] [%]
1	Oil-bath in ethanol	80	120	75
2	MW in ethanol	80	7	87
3	MW in ethanol	100	4	85
4	MW without ethanol	80	7	36
5	MW without ethanol	80	20	80

[a] Isolated yields.

Synthesis

Ligand **L** was synthesized from the parent rhodamine B and 2-pyridinecarboxaldehyde in a two-step process described above (Scheme 2) using microwave heating protocols and conventional oil-bath, by adapting the procedure reported in the literature (in ESI†).[5,24]

Step I: Synthesis of rhodamine B hydrazide (2). *Using microwave heating protocol*: A mixture of rhodamine B **1** (0.12 g, 0.25 mmol), an excess of hydrazine hydrate (80%) (0.3 mL) and ethanol (3 mL) was placed in a 10 mL reaction vial. Alternatively, the reaction can be performed without ethanol using a slight excess of hydrazine hydrate (80%) (0.5 mL). The resulting mixture was stirred to make it homogeneous and it was placed in the cavity of a CEM microwave reactor. The reaction was irradiated according to the parameters described in Table 1. After cooling to room temperature, the resulting solid was filtered and washed 3 times with water. After drying, the rhodamine B hydrazide (**2**) was isolated to give the yields presented in Table 1. ^{1}H-NMR ($CDCl_3$), δ (ppm): 1.14 (12 H, t, J = 7.2 Hz, NCH_2CH_3), 3.31 (8 H, q, J = 7.2 Hz, NCH_2CH_3), 3.64 (2 H, broad s, NH_2), 6.31 (2 H, dd, J = 8.8 and J = 2.4 Hz, H-2, 7), 6.44 (2 H, d, J = 2.4 Hz, H-4, 5), 6.48 (2 H, d, J = 8.8 Hz, H-1, 8), 7.12–7.14 (1 H, m, Ar-H), 7.46–7.50 (2 H, m, Ar-H), 7.95–7.97 (1 H, m, Ar-H).

Step II: Synthesis of ligand (L). *Using microwave heating protocol*: A mixture of rhodamine B hydrazide **2** (30 mg, 66 μmol), 2-pyridinecarboxaldehyde (0.05 mL, 0.53 mmol) and ethanol (2 mL) was placed in a 10 mL reaction vial. Alternatively, the reaction can be performed without ethanol using the same amount of 2-pyridinecarboxaldehyde (0.05 mL, 0.53 mmol). The resulting mixture was stirred to make it homogeneous and it was placed in the cavity of a CEM microwave reactor. The reaction was irradiated according to the parameters described in Table 2. After cooling to room temperature, the resulting solid was filtered and washed 3 times with cold ethanol. After drying, the ligand (**L**) was isolated to give the yields presented in Table 2. ^{1}H-NMR ($CDCl_3$), δ (ppm): 1.14 (12 H, t, J = 7.2 Hz, NCH_2CH_3), 3.31 (8 H, q, J = 7.2 Hz, NCH_2CH_3), 6.23 (2 H, dd, J = 8.8 and J = 2.8 Hz, H-2, 7), 6.45 (2 H, d, J = 2.8 Hz, H-4, 5), 6.55 (2 H, d, J = 8.8 Hz, H-1, 8), 7.10–7.15 (2 H, m, H-Ar), 7.44–7.49 (2 H, m, H-Ar), 7.61 (1 H, dt, J = 7.6 and J = 1.6 Hz, H-Ar), 8.00–8.02 (2 H, m, H-Ar), 8.37 (1 H, s, N=C–H), 8.46–8.47 (1 H, dd, J = 4.0 and J = 0.8 Hz, H_{ortho}-pyridyl). ^{13}C-NMR ($CDCl_3$), δ (ppm): 12.8 (NCH_2CH_3), 44.4 (NCH_2CH_3), 66.0 (spiro carbon), 98.4 (C-4, 5), 105.7 (C-1a, 8a), 108.2 (C-2, 7), 120.8, 123.7, 123.8, 123.9, 127.7 (C-1, 8), 128.1, 128.4, 133.9, 136.2, 146.0 (N=C–H), 149.1, 149.2, 152.7, 153.0, 154.8, 165.6 (C=O). ESI mass spectrometry: m/z 568 $[M + Na]^+$, 546 $[M + H]^+$. Anal. calcd for $C_{34}H_{35}N_5O_2$: C, 74.84, N, 12.83, H, 6.47. Found: C, 74.47, N, 12.80, H, 6.23.

Table 2 Step II experiments to prepare ligand (**L**) using different heating methods

Entry	Method	Temp. [°C]	Time (min)	Yield[a] [%]
1	Oil-bath in ethanol	80	360	57
2	MW in ethanol	80	10	58
3	MW in ethanol	100	8	87
4	MW without ethanol	80	10	70

[a] Isolated yields.

Single-crystal X-Ray diffraction

A crystal suitable for single-crystal X-ray diffraction analysis of the ligand **L** was manually harvested and mounted on a Hampton Research CryoLoop using FOMBLIN Y perfluoropolyether vacuum oil (LVAC 25/6).[25] Data were collected at room temperature on a Bruker X8 Kappa APEX II Charge-Coupled Device (CCD) area-detector diffractometer (Mo K_α graphite-monochromated radiation was used, λ = 0.71073 Å) with the crystal positioned at 35 mm from the detector and using 10 s of exposure time. The acquisition was controlled by the APEX2 software package,[26] the images were processed with the software SAINT+,[27] and absorption correction was performed by the multi-scan semi-empirical method implemented in SADABS.[28] The structure was solved by the direct methods of SHELXS-97,[29,30] with all the non-hydrogen atoms located from difference Fourier maps calculated from successive full-matrix least-squares refinement cycles on F^2 using SHELXL-97, and being successfully refined with anisotropic displacement parameters.[30,31]

Hydrogen atoms bonded to carbons of the ligand **L** were located at their geometrical positions using appropriate HFIX instructions in SHELXL (43 for the aromatic groups, 23 for the $-CH_2-$ groups and 137 for terminal $-CH_3$ groups) and included in subsequent refinement cycles in riding-motion approximation with isotropic thermal displacement parameters (U_{iso}) fixed at 1.2 × U_{eq} (for the aromatic and CH_2 groups) and 1.5 × U_{eq} (for the methyl group) of the carbon atom to which they are attached. The last difference Fourier map synthesis revealed the highest peak (0.45 e $Å^{-3}$) and deepest hole (−0.31 e $Å^{-3}$) located at 1.12 Å from C4 and 0.58 Å from C3, respectively.

Crystal data for **L**: $C_{34}H_{35}N_5O_2$, M = 545.67, monoclinic, space group $P2_1/c$, a = 9.457(4) Å, b = 26.104(14) Å, c = 12.077(6) Å, α = 90°, β = 103.449(15)°, γ = 90°, V = 2900.0(2) $Å^3$, room temperature, Z = 4, μ = 0.079 mm^{-1}, $\rho calc$ = 1.250 g cm^{-3}, orange prism crystal with 0.19 × 0.11 × 0.05 mm^3; 23 629 reflections measured with 4984 being independent (R_{int} = 0.0522); the final R_1 and w$R(F^2)$ values were 0.0683 [$I > 2\sigma(I)$] and 0.1932 (all data), respectively; data completeness to θ = 25.03°, 97.3%; CCDC 901532.

Absorption and fluorescence spectroscopic measurements

Absorption spectra were acquired with a Shimadzu UV-3600 spectrophotometer equipped with a constant-temperature cell holder, at 25 °C, in 1 cm cuvettes, in the wavelength range 450–1100 nm.

Fluorescence measurements were performed in a Varian Cary Eclipse fluorimeter, equipped with a constant-temperature cell holder, at 25 °C, in 1 cm cuvettes. Spectra were recorded with excitation and emission slit widths of 5 nm, 600 V of voltage and with λ_{exc} = 556 nm and λ_{em} from 566–700 nm for compound **L** and the respective iron(III) complex. To minimize reabsorption effects, the absorbance's sample values were kept below 0.1.

A stock solution of compound **L** was prepared from a concentrated solution of the compound in dimethylsulfoxide (DMSO). Samples for absorption and fluorescence measurements were prepared by dilution of the appropriate volume of the DMSO stock solution. Aqueous solutions were prepared from the stock solution and the percentage of the DMSO in the final solutions was always less than 1%.

Fluorescence spectra of L at variable pH

All solutions were prepared with double de-ionized water (conductivity less than 0.1 μ Scm^{-1}).

For the spectroscopic data the pH values were measured on a Crison pH meter Basic 20+ equipped with a combined glass electrode and it was standardized at 25 °C by using standard buffers of pH 4, 7 and 9. The fluorescence spectra obtained to determine log K_a values were recorded, at each pH, using the fluorimeter already described. Stock solutions of the ligand were prepared in water (I = 0.1 M NaCl). For variable pH measurements in the range 1.5 < pH < 10 we started from a solution prepared as described and aliquots of strong base or acid were added to adjust the pH to the desired value. After each pH adjustment the solution was transferred into the cuvette, and the fluorescence spectra were recorded. Spectra were acquired at 25 °C and between 566 and 700 nm (1 nm resolution). The pK_a values were calculated using the program HypSpec™.[32,33] The errors associated were calculated by the method suggested by Albert and Sergeant.[34] The distribution diagrams were plotted with the HySS program.[35] The calculations were performed with data from at least four independent measurements, each with 31 spectra in the pH range 1.5 < pH < 10.

Evaluation of the interaction of the ligand L with Fe^{3+}

The evaluation of the interaction of ligand **L** with iron(III) was performed in DMSO and DMSO–H_2O at 25 °C. A stock solution of $Fe(NO_3)_3$ was prepared from the respective salt in DMSO. Concentrated solutions of **L** in DMSO were prepared and used as stock solutions.

Electronic spectra were recorded under two different experimental conditions in order to assess the influence of solvent and time.

(1) Several solutions containing the ligand **L** and the corresponding amount of metal ion stock solution to achieve a (**L** : Fe^{3+}) ratio of 1 : 0.6 were prepared both in DMSO and DMSO–H_2O (90% : 10%). UV-Vis spectra were acquired at variable intervals of time during 24 hours.

(2) Solutions of ligand **L** were prepared both in DMSO and in DMSO–H_2O (90% : 10%). To each solution, increasing amounts of the metal ion stock solution were added in order to achieve a (**L** : Fe^{3+}) ratio ranging from 1 : 0.01 to 1 : 1. UV-Vis spectra were acquired upon each addition.

The solutions for fluorescence measurements were prepared by dilution of the solutions used to obtain the UV-Vis spectra in order to obtain solutions with absorbance below 0.1 to minimize reabsorption effects.

Results and discussion

The classical synthetic protocol to synthesize ligand **L** involves the reaction of rhodamine B **1** with hydrazine hydrate (80%) in ethanol (step I), followed by condensation of the resulting rhodamine B hydrazide **2** with 2-pyridinecarboxaldehyde also in ethanol (step II), as is described in Scheme 2. This protocol is based on conventional round-bottomed flask chemistry, and the overall reaction time is 480 min (8 h) to obtain an overall yield of 43% (see Table 1, entry 1 and Table 2, entry 1).

In order to explore a simplified, less time-consuming, and high-yielding procedure, we have considered the use of controlled microwave heating under closed-vessel conditions to optimize the reaction conditions. Recently, G. Song and coworkers have established an efficient and rapid method to synthesize aryl and alkyl hydrazides from the reaction of esters with hydrazine monohydrate using microwave, ultrasound and simultaneous microwave and ultrasound irradiation, respectively.[36] Curiously, all these reactions were conducted under open-vessel conditions, at atmospheric pressure. In this work

we explored the use of the microwave closed-vessel conditions to reach rhodamine B hydrazide **2**, and perform its conversion into ligand **L**.

First experiments to synthesize **2** employed closed-vessel microwave conditions (80 °C) and resulted in better yields (87%) within a slightly reduced reaction time (7 min) (Table 1, entry 2). By increasing the reaction temperature to 100 °C, the reaction took place in only 4 min, affording **2** in 85% yield (Table 1, entry 3). In the context of sustainable synthetic chemistry, the aim is not only to seek for methods of more efficient heating but also to develop methods that avoid the use of organic solvents and other auxiliary agents. Experiments without ethanol were carried out (80 °C, 7 min) giving **2** in only 36% yield (64% of the starting rhodamine **1** was recovered unchanged) (Table 1, entry 4). To reach full reaction conversion at 80 °C, the reaction time was extended to 20 min affording **2** in 80% yield (Table 1, entry 5).

The conversion of **2** into ligand **L** was achieved in only 10 min at 80 °C, affording **L** in 58% yield (Table 2, entry 2) using the microwave close-vessel conditions protocol. The yield was also improved to 87% by raising reaction temperature to 100 °C and reducing time to 8 min (Table 2, entry 3). Full reaction conversion was achieved without ethanol (80 °C, 10 min), affording the extended ligand **L** in 70% yield (Table 2, entry 4).

These results reveal that the microwave irradiation protocol significantly accelerates the synthesis of ligand **L**, resulting in successful completion of the two reactions in only 30 min, to obtain an overall yield of 56%, without the use of any organic solvent.

The ^{1}H NMR spectra of ligand **L** show the typical aromatic group of signals of the xanthene scaffold, which are: (i) the double doublet at 6.23 Hz assigned to the resonance of 2-H and 7-H, (ii) the doublet at 6.45 Hz corresponding to the resonance of 4-H and 5-H and (iii) the doublet at 6.55 Hz due to the resonance of 1-H and 8-H. Relatively more de-shielded appear the signals from the protons of the substituted phenyl and pyridyl rings. 1-H and 8-H show HMBC correlation with a signal at 66.0 ppm assigned to a spiro carbon atom. This value at 66.0 ppm provides evidence of the presence of the rhodamine in the spirolactam form and is consistent with the values described in the literature for these compounds.[17,23]

The crystal structure of the ligand **L** (Fig. 1a) unequivocally confirms the spirolactam-ring configuration (spiro atom C20). Recrystallization from ethanol resulted in crystals suitable for single-crystal X-ray diffraction studies, which allowed the crystal structure determination. **L** crystallized in the monoclinic system and the structure was solved and refined in the $P2_1/c$ space group, with the asymmetric unit revealing only one entire molecule without any crystallization solvent. As observed in similar compounds,[37–43] the xanthene moiety is practically orthogonal to the benzene spirolactam-ring group and to the pyridine ring, with the dihedral angle between mean planes of 88.02(6)° and 88.97(9)°, respectively (see Fig. S1 in ESI†). The structural conformation of ligand **L** and its crystalline packing arrangement are definitely conditioned

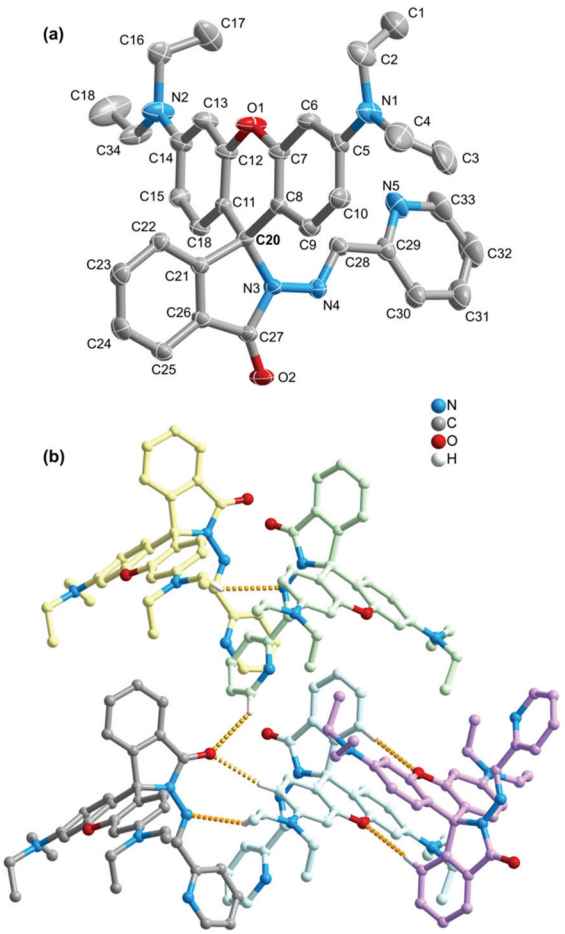

Fig. 1 (a) Crystal structure of the spirolactam form of **L**; hydrogen atoms were omitted for clarity reasons and displacement ellipsoids were drawn at 25% of probability. (b) C–H···O and C–H···N weak hydrogen bond interactions (orange dashed lines) between five adjacent **L** molecules; for clarity reasons the C-atoms of distinct molecules are represented in different colours and only the H-atoms directly involved in intermolecular interactions are drawn.

Table 3 Geometry details of the C–H···X hydrogen bonds found in the crystalline structure of ligand **L** (distances in Å and angles in degrees)

C–H···X	d(H···X)	d(C···X)	<(CHX)
C22–H22···O1^{i}	2.615(2)	3.545(6)	179(1)
C15–H15···O2^{ii}	2.462(3)	3.343(5)	158(1)
C33–H33···O2^{iii}	2.618(2)	3.388(6)	140(1)
C34–H34A···N4^{ii}	2.695(3)	3.537(6)	146(1)

Symmetry transformations used to generate equivalent atoms: (i) $-x$, $1-y$, $-z$; (ii) x, $3/2-y$, $-1/2+z$; (iii) $-1+x$, $3/2-y$, $-1/2+z$.

and stabilized by an extensive network of intermolecular interaction, particularly C–H···O and C–H···N weak hydrogen bonds (Fig. 1b) and Table 3). While the H···O distances range from 2.463(3) to 2.618(2) Å, the H···N distances are slightly longer, 2.695(3) Å. This extensive network of weak intermolecular interaction reinforces the dense crystalline packing arrangement of ligand **L** (Fig. S2 in ESI†).

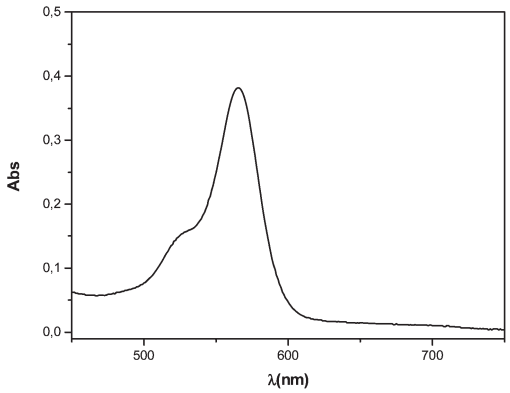

Fig. 2 UV-Vis spectrum of ligand **L** in water, at pH = 2.70.

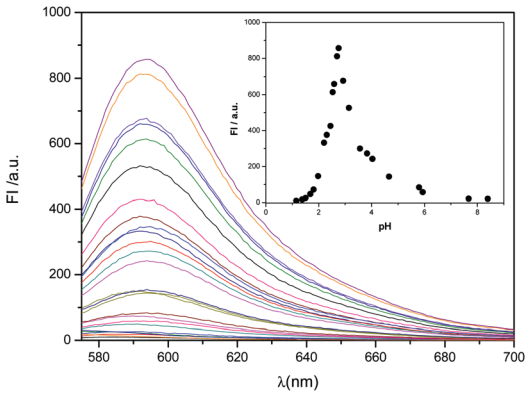

Fig. 3 Variation of the fluorescence intensity of **L** (1.61×10^{-5} M) in water with pH.

Studies in aqueous solution and at variable pH

Dilution in water of a concentrated stock solution of **L** in DMSO, to yield a concentration of 8.06×10^{-5} M (the percentage of DMSO is less than 1%), results in an aqueous solution of pH equal to 2.70 that exhibits the UV-Vis spectrum depicted in Fig. 2. The spectrum presents the profile expected for ligands with a rhodamine moiety exhibiting an absorption band with a λ_{abs} = 565 nm, with a $\varepsilon_{(water)}$ = 4739 mol dm^{-3} cm^{-1}.

Starting from this solution and raising the pH we observed that the compound starts to precipitate at pH equal to 3.0 thus implying the choice of another concentration range to determine the acidity constants. Using this information and a lower concentration, 1.61×10^{-5} M, a fluorescence profile of the ligand **L** was obtained in water in the pH range 1.5 < pH < 10. The results obtained are shown in Fig. 3.

The spectral data obtained and analysed with the program HypSpec are consistent with the presence of three species (H_2L^{2+}, HL^+, L) along pH and allowed the determination of two pK_a values, which are listed in Table 4. The two values are very close and lower than those reported in the literature for this family of ligands.[44] In particular, the value of pK_{a2} is lower than 3 and consequently the non-fluorescent species L is predominant above pH 4, a property which is advantageous for discrimination of the origin of fluorescence turn-on in the presence of metal ions.[45]

Table 4 Acidity constants of **L**

pK_{ai}	Ligand **L** (H_2L^{2+})
pK_{a1}	2.89 ± 0.01
pK_{a2}	2.98 ± 0.03

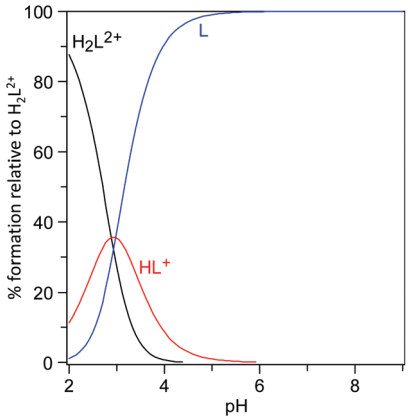

Fig. 4 Speciation diagram for **L**, as a function of pH.

The speciation diagram of ligand **L** along pH is depicted in Fig. 4 in the range 2 < pH < 9. Due to the proximity of the two pK_a values, the three species (H_2L^{2+}, HL^+, L) are present in solution in the range 2 < pH < 4. For pH values above 4 the non-protonated form is predominant and above pH 6 the molar fraction of **L** is equal to one thus indicating that **L** is the sole species in solution. The formulae of the three species in which **L** may be present are indicated in Scheme 3.

Analysing the fluorescent properties of the three species it can be seen that only the monoprotonated form, HL^+, is fluorescent. The latter is assigned to the ring-opened form, and the diprotonated form, H_2L^{2+}, a non-fluorescent form, to a species protonated at the pyridyl ring. This protonation introduces fluorescence quenching properties in the pyridinium ring by means of photoinduced electron transfer.[46]

As a consequence of the two very low pK_a values:

(i) The maximum fluorescence intensity is observed at pH = 3. The predominant species in solution is HL^+.

(ii) At pH = 4 only 5% of HL^+ is present in solution and the predominant species in solution is the non-fluorescent form L.

(iii) At pH = 5 only the non-fluorescent species L is present in solution.

Considering the above properties, this ligand may be of use to detect pH changes in the range 2 < pH < 4. The most advantageous property seems to be the possibility of assuring that at pH above 4 there is no interference of pH in the opening of the spirolactam form and the fluorescence 'turn-on' thus allowing the confident analysis of the interaction of metal ions.

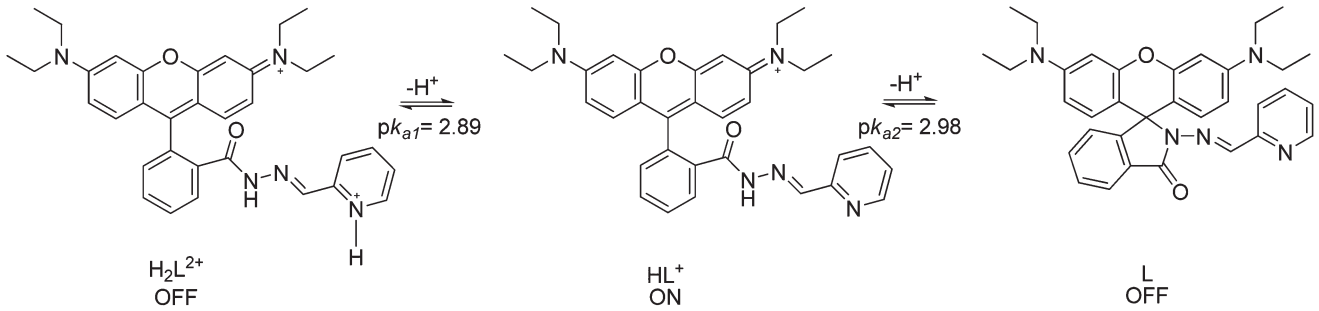

Scheme 3 Dissociation steps of the ligand **L**.

Interaction of L with Fe^{3+}

In order to assess the possibility of using compound **L** to monitor iron, the interaction of **L** with Fe^{3+} was investigated by examining the variation in the absorption spectra of solutions containing ligand **L** in DMSO and DMSO–H_2O. The study of the interaction of the ligand with iron(III) was performed in DMSO and DMSO–H_2O to disregard the influence of pH and the low solubility of the compound. Since **L** is a tridentate ligand we used a 1 : 0.6 ligand to metal ratio in order to grant quantitatively formation of the complex. This coordination involves the two nitrogen atoms (the deprotonated N4 nitrogen of the picolylimine and the N5 of the pyridine ring), and one oxygen atom of the rhodamine spirolactam form. The spectra were acquired at variable intervals of time during 24 hours. The behaviour along time was different in DMSO and in DMSO–H_2O.

In pure DMSO solution the intensity of the rhodamine band (λ_{abs} = 565 nm) varies gradually and the maximum value stabilizes after t = 120 min, while for DMSO–H_2O a maximum intensity is achieved at t = 60 min. The charge transfer band λ_{abs} = 600–700 nm, assigned to the iron complex, is visible after 24 hours in both cases.[44]

In Fig. 5 we show the UV-Vis spectra of the prepared solution after (A) t = 60 min for the DMSO solution, t = 120 min for the DMSO–H_2O solution (B) for 24 h of stabilization for both solutions.

Considering the previous results, we studied the variations observed in the maximum of the absorption wavelength for ligand **L** solutions in DMSO–H_2O after addition of increasing amounts of iron(III) (Fig. 6), to confirm the formation of the FeL_2 complex.

The curve clearly indicates that as the concentration of Fe^{3+} is raised the maximum of the absorbance intensity band increases until the ligand : metal ratio reaches 1 : 0.5, which is in agreement with the fact that this ligand acts as a tridentate ligand.

The interaction of ligand **L** with Fe^{3+} was also followed by fluorescence. After 24 hours stabilization spectra of ligand **L**, and ligand **L** : Fe^{3+} (1 : 0.6) were acquired in DMSO and in DMSO–H_2O, as depicted in Fig. 7.

The fluorescence spectra show that ligand **L** is non-fluorescent while its iron complex exhibits a strong fluorescence band at λ_{em} = 586 nm. However fluorescence intensity is *ca.* 10 times higher in DMSO–H_2O.

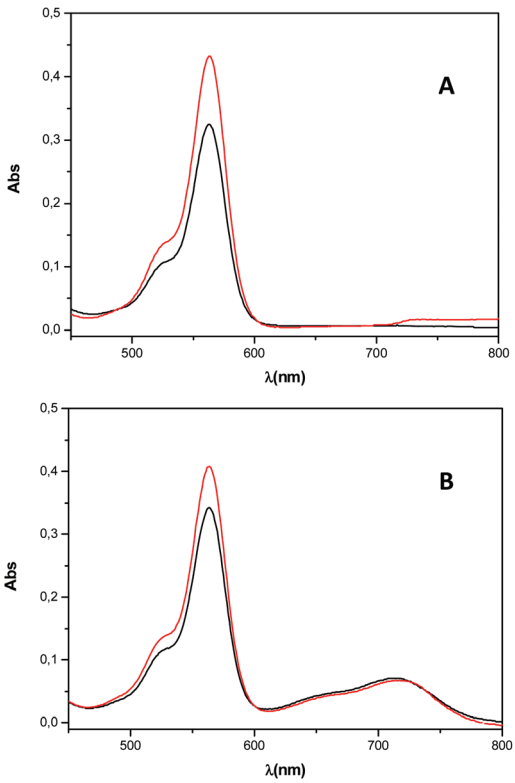

Fig. 5 UV-Vis spectra of **L** : Fe^{3+} (1 : 0.6) (A) t = 60 min for the DMSO–H_2O solution (red line), t = 120 min for the solution DMSO (black line), and (B) DMSO (black line) and DMSO–H_2O (90% : 10%) (red line) after 24 hours.

Bearing in mind the potential application of this ligand in cellular media we investigated the behaviour of the ligand in the presence of other relevant metal ions, Zn(II), Fe(II), Cu(II). The results show that only Cu(II) triggers the opening of the spirolactam form of ligand **L** (Fig. S3 in ESI†), as reported previously.[23] However, considering the total concentration of both ions in the cellular media we assume that copper(II) will not interfere in the complexation of iron(III).[47,48]

We intend to further investigate the complexation properties of ligand **L** with iron(III) and copper(II) in order to assess

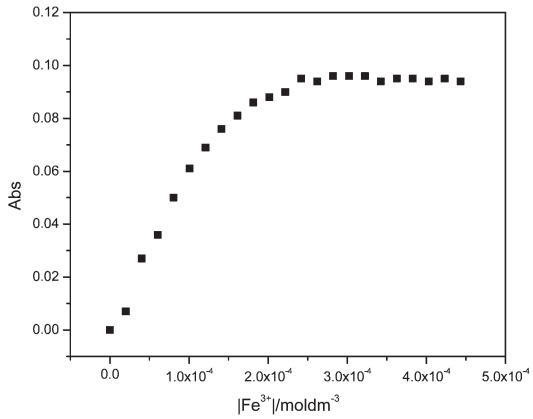

Fig. 6 Variation in the maximum of the absorption wavelength of ligand **L** (DMSO–H_2O (90% : 10%), 25 °C) with increasing concentration of iron(III).

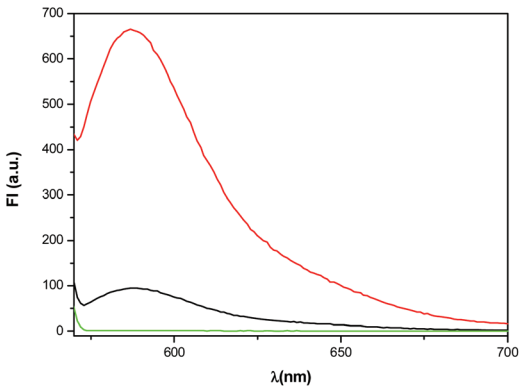

Fig. 7 Variation of the fluorescence intensity of **L** in DMSO (green line) with the addition of Fe^{3+}, in DMSO (black line), DMSO–H_2O (90% : 10%) (red line).

the values of the corresponding stability constants and perform competition studies to establish the experimental conditions in which the ligand allows confident determination of iron(III) and copper(II).

Conclusions

In this work we report the first example of a 'turn-on' fluorescent ligand based on rhodamine B prepared using microwave-assisted synthesis and without the use of any organic solvent. Full characterization of ligand **L** is presented including the single crystal X-ray structure and speciation in aqueous solution. The ligand exhibits two very low pK_a values which allow the discrimination between its fluorescent monoprotonated form (HL^+) and its iron(III) complex, above pH 4. The coordination of iron(III) induces the opening of the spirolactam ring and triggers a turn-on fluorescence effect, observation of a strong fluorescence band at λ_{em} = 586 nm, upon formation of the complex.

Acknowledgements

This work was supported by Fundação para a Ciência e a Tecnologia through projects PTDC/SAU-MET/113011/2009 and PEst-C/EQB/LA0006/2011. We thank Dr Andrea Carneiro from CeNTI, V.N. Famalicão, for making available to us a CEM Discover microwave reactor. The Bruker Avance II 400 spectrometer is part of the National NMR network and was purchased under the framework of the National Programme for Scientific Re-equipment, contract REDE/1517/RMN/2005, with funds from POCI 2010 (FEDER) and (FCT).

References

1 D. W. Domaille, E. L. Que and C. J. Chang, *Nat. Chem. Biol.*, 2008, **4**, 168–175.
2 S. S. Tan, S. J. Kim and E. T. Kool, *J. Am. Chem. Soc.*, 2011, **133**, 2664.
3 X. Chen, T. Pradhan, F. Wang, J. S. Kim and J. Yoon, *Chem. Rev.*, 2012, **112**, 1910.
4 V. Dujols, F. Ford and A. W. Czarnik, *J. Am. Chem. Soc.*, 1997, **119**, 7386.
5 X.-F. Yang, X.-Q. Guo and Y.-B. Zhao, *Talanta*, 2002, **57**, 883.
6 H. N. Kim, M. H. Lee, H. J. Kim, J. S. Kim and J. Yoon, *Chem. Soc. Rev.*, 2008, **37**, 1465.
7 L. Tang, J. Guo, Y. Cao and N. Zhao, *J. Fluoresc.*, 2012, **22**, 1603.
8 Z. Xua, L. Zhang, R. Guo, T. Xiang, C. Wu, Z. Zheng and F. Yang, *Sens. Actuators, B*, 2011, **156**, 546.
9 L. Tanga, F. Li, M. Liu and R. Nandhakumar, *Spectrochim. Acta, Part A*, 2011, **78**, 1168.
10 M. Dong, T.-H. Ma, A.-J. Zhang, Y.-M. Dong, Y.-W. Wang and Y. Peng, *Dyes Pigm.*, 2010, **87**, 164.
11 X. Chen, M. J. Jou, H. Lee, S. Kou, J. Lim, S.-W. Nam, S. Park, K.-M. Kim and J. Yoon, *Sens. Actuators, B*, 2009, **137**, 597.
12 K. M. K. Swamy, S.-K. Ko, S. K. Kwon, H. N. Lee, C. Mao, J.-M. Kim, K.-H. Lee, J. Kim, I. Shin and J. Yoon, *Chem. Commun.*, 2008, 5915.
13 C. Yu, J. Zhang, R. Wang and L. Chen, *Org. Biomol. Chem.*, 2010, **8**, 5277.
14 Y. Xiang and A. Tong, *Luminescence*, 2008, **23**, 28.
15 Y. Zhou, J. Zhang, H. Zhou, Q. Zhang, T. Ma and J. Niu, *Sens. Actuators, B*, 2012, 508.
16 H. Yang, Z. Zhou, K. Huang, M. Yu, F. Li, T. Yi and C. Huang, *Org. Lett.*, 2007, **9**, 4729.
17 M. Zhang, Y. Gao, M. Li, M. Yu, F. Li, L. Li, M. Zhu, J. Zhang, T. Yia and C. Huang, *Tetrahedron Lett.*, 2007, **48**, 3709.
18 Y. Liu, Y. Sun, J. Du, X. Lv, Y. Zhao, M. Chen, P. Wang and W. Guo, *Org. Biomol. Chem.*, 2011, **9**, 432.
19 M. Zhao, X.-F. Yang, S. He and L. Wang, *Sens. Actuators, B*, 2009, **135**, 625.

20 X. Chen, X. Wang, S. Wang, W. Shi, K. Wang and H. Ma, *Chem.–Eur. J.*, 2008, **14**, 4719.
21 L. Mei, Y. Xiang, N. Li and A. Tong, *Talanta*, 2007, **72**, 1717.
22 C. O. Kappe and D. Dallinger, *Mol. Diversity*, 2009, **13**, 71.
23 N. R. Chereddy, K. Suman, P. S. Korrapati, S. Thennarasu and A. B. Mandal, *Dyes Pigm.*, 2012, **95**, 606–613.
24 Y. Xiang, A. Tong, P. Jin and Y. Ju, *Org. Lett.*, 2006, **8**, 2863.
25 T. Kottke and D. Stalke, *J. Appl. Crystallogr.*, 1993, **26**, 615.
26 *APEX2, Data Collection Software Version 2.1-RC13*, Bruker AXS, Delft, The Netherlands, 2006.
27 *SAINT+, Data Integration Engine v. 7.23a ©*, Bruker AXS, Madison, Wisconsin, USA, 1997–2005.
28 G. M. Sheldrick, *SADABS v.2.01, Bruker/Siemens Area Detector Absorption Correction Program*, Bruker AXS, Madison, Wisconsin, USA, 1998.
29 G. M. Sheldrick, *SHELXS-97, Program for Crystal Structure Solution*, University of Göttingen, 1997.
30 G. M. Sheldrick, *Acta Crystallogr., Sect. A: Fundam. Crystallogr.*, 2008, **64**, 112.
31 G. M. Sheldrick, *SHELXL-97, Program for Crystal Structure Refinement*, University of Göttingen, 1997.
32 P. Gans, A. Sabatini and A. Vacca, *Talanta*, 1996, **43**, 1739.
33 P. Gans, A. Sabatini and A. Vacca, *Annali di chimica*, 1999, **89**, 45.
34 A. Albert and E. Sergeant, *The Determination of Ionization Constants*, Chapman and Hall Ltd, Londres, 2nd edn, 1971.
35 L. Alderighi, P. Gans, A. Ienco, D. Peters, A. Sabatini and A. Vacca, *Coord. Chem. Rev.*, 1999, **184**, 311.
36 Y. Peng and G. Song, *Green Chem.*, 2001, **3**, 302.
37 X. Chen, X. Wang, S. Wang, W. Shi, K. Wang and H. Ma, *Chem.–Eur. J.*, 2008, **14**, 4719.
38 A. J. Weerasinghe, C. Schmiesing and E. Sinn, *Tetrahedron Lett.*, 2009, **50**, 6407.
39 Y. Zhou, F. Wang, Y. Kim, S.-J. Kim and J. Yoon, *Org. Lett.*, 2009, **11**, 4442.
40 W. Zhang, B. Tang, X. Liu, Y. Liu, K. Xu, J. Ma, L. Tong and G. Yang, *Analyst*, 2009, **134**, 367.
41 A. J. Weerasinghe, C. Schmiesing and E. Sinn, *Tetrahedron*, 2011, **67**, 2833.
42 H. N. Kim, S.-W. Nam, K. M. K. Swamy, Y. Jin, X. Chen, Y. Kim, S.-J. Kim, S. Park and J. Yoon, *Analyst*, 2011, **136**, 1339.
43 W.-Y. Liu, H.-Y. Li, B.-X. Zhao and J.-Y. Miao, *Org. Biomol. Chem.*, 2011, **9**, 4802.
44 P. V. Bernhardt, P. Chin, P. C. Sharpe, J.-Y. C. Wang and D. R. Richardson, *J. Biol. Inorg. Chem.*, 2005, **10**, 761.
45 J. D. Chartres, M. Busby, M. J. Riley, J. J. Davis and P. V. Bernhardt, *Inorg. Chem.*, 2011, **50**, 9178.
46 P. P. Laine, S. Campagna and F. Loiseau, *Coord. Chem. Rev.*, 2008, **252**, 2552.
47 T. D. Rae, P. J. Schmidt, R. A. Pufahl, V. C. Culotta and T. V. O'Halloran, *Science*, 1999, **284**, 805.
48 H. Glickstein, R. Ben El, M. Shvartsman and Z. I. Cabantchik, *Blood*, 2005, **106**, 3242.

